J Mater Sci: Mater Med (2012) 23:2709–2716
DOI 10.1007/s10856-012-4728-x

Electrospun emodin polyvinylpyrrolidone blended nanofibrous membrane: a novel medicated biomaterial for drug delivery and accelerated wound healing

Xin-Yi Dai · Wei Nie · Yong-Chun Wang · Yi Shen · Yan Li · Shu-Jie Gan

Received: 28 January 2012 / Accepted: 23 July 2012 / Published online: 9 August 2012

Abstract In this work, blended nanofibrous membranes were prepared by an electrospinning technique with polyvinylpyrrolidone (PVP) K90 as the filament-forming polymer, and emodin, an extract of polygonum cuspidate known as a medicinal plant, as the treatment drug. Detailed analysis of the blended nanofibrous membrane by scanning electron microscopy, Differential scanning calorimetry and X-ray diffraction revealed that emodin was well distributed in the ultrafine fibers in the form of amorphous nanosolid dispersions. Results from attenuated total reflectance Fourier transform infrared spectra suggested that the main interactions between PVP and emodin might be mediated through hydrogen bonding. In vitro dissolution tests proved that the blended nanofibrous membrane produced more desired release kinetics of the entrapped drug (emodin) as compared to the pure drug. Furthermore, wound healing test and histological evaluation revealed that the emodin loaded nanofibrous membrane to be more effective as a healing accelerator thereby proving potential strategies to develop composite drug delivery system as well as promising materials for future therapeutic biomedical applications.

X.-Y. Dai (✉) · Y.-C. Wang
Division of Plastic Surgery, Shanghai Jiaotong University Affiliate First People Hospital, Shanghai 200080, China
e-mail: daixy1979@gmail.com

W. Nie
Key Laboratory of Targeting Agents, Fudan University, Shanghai 200433, China

Y. Shen
Shanghai Center for Systems Biomedicine, Shanghai Jiao Tong University, Shanghai 201800, China

Y. Li
Division of Intensive Care Unit, Shanghai Jiaotong University Affiliate First People Hospital, Shanghai 200080, China

S.-J. Gan
Division of Vascular Surgery, Shanghai Jiaotong University Affiliate First People Hospital, Shanghai 200080, China

1 Introduction

Acute wound exists in all patients underwent surgical procedures or with trauma. In the United States alone, approximately 50 million surgical procedures are performed each year and the need for postsurgical wound care is sharply on the rise with the expectation to reach more than 38.0 million by 2012. Moreover, fifty million additional traumatic wounds add to the burden of acute wound morbidity [1, 2].These wounds are posing critical clinical challenges. Although surgical interventions such as free flap transfer may achieve some improvements, those operative procedures, representing the only solution to heal tissue defects, are often followed by donor site morbidity and subsequent loss of function, let alone severe complications such as flap compromise [3]. Therefore, noninvasive wound management via topical administration of pro-healing agents restored in a biocompatible dressing materials that can create and maintain an optimal wound healing environment has become popular and proven to be effective [4]. Recently, nanofibrous nonwoven membranes as drug delivery systems produced by an electrospinning process have been shown great potential and therefore has become the focus of attention [5, 6]. This simple, versatile and useful technique has made it available to produce ultrafine fibers from polymer solutions with diameters in the range of nanometer to sub-micrometers [7], which in turn, to fabricate porous, nanofibrous structured membranes that bare favorable properties for wound dressing

such as excellent oxygen permeability, maintenance of a moist environment, protection against microorganism, conformation to the wound surface and the potential for leaving no scar [8, 9]. A particular advantage of this delivery system would be the possibility of delivering uniform, high, controlled doses of bioactive agents at the wound site, which is also based on its unique structural and physical properties: (1) the extraordinary high surface area per unit mass of the fibers facilitates fast release of the restored active ingredients; (2) fibrous membranes have high porosity and the selected drug can exist in electrospun nanofibers in an amorphous state or as nanocrystals, which can be very useful for increasing both the solubility and the dissolution rate of poorly water-soluble drugs [4, 6].

Emodin (1,3,8-trihydroxy-6-methyl-anthraquinone, Fig. 1a) is an anthraquinone derivative from the roots of Polygonum cuspidate (Chinese name Huzhang), a Chinese herb that has been widely used for the treatment of suppurative dermatitis, gonorrhea, arthralgia and so on [10]. The reported biological effects of emodin include anti-inflammatory, antibacterial and enhance the nucleotide excision repair of DNA damage in human cells [11]. Recently, study indicates that emodin also has the ability to accelerate wound healing which is related to TGF-β1/Smad signaling pathway [12].

As an aid to increase the solubility of drugs and as an inhibitor of recrystallisation, Polyvinylpyrrolidone (PVP, Fig. 1b) is another important polymer commonly used in medical or pharmaceutical industries [13, 14]. The U.S. Food and Drug Administration has approved this chemical for a wide variety of applications and it is generally considered safe. Due to its well spinnable and water soluble feature, electrospun PVP fibers have already been used to load various drug for improving their bioavailability [15, 16].

In this study, we demonstrated the utility of a novel polymeric, nanofiber based drug delivery system—emodin/PVP electrospun nanofibrous membrane as a topical wound healing agent in treating acute full-thickness skin wound in a mouse model.

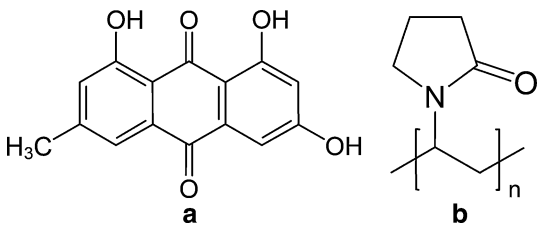

Fig. 1 Chemical structure: **a** emodin (1,3,8-trihydroxy-6-methyl-anthraquinone), **b** PVP

2 Materials and methods

2.1 Materials

PVP (K90, M = 360,000 Da) was purchased from Shanghai Yunhong Pharmaceutical Aids and Technology Co., Ltd (Shanghai, China). The dried roots of polygonum cuspidate were provided by Shanghai Chen-shan Botanical Garden (Shanghai, China). Anhydrous ethanol was provided by Sinopharm Chemical Reagent Co., Ltd (Shanghai, China). All other chemicals used were analytical grade. Water was double distilled just before use.

2.2 Extraction and purification of emodin

Our protocol to extract and purification emodin from polygonum cuspidate is based on previous literature [17].

2.3 Preparation of spinning solution

All electrospinning processes were performed at ambient conditions (temperature 24–25 °C and relative humidity ~65 %). Emodin and PVP K90 were dissolved in ethanol in turn. The concentration of PVP was fixed at 10 (w/v) % while the concentration of emodin was 0.2 (w/v) %, meaning drug-to-PVP weight ratios of 2:100 in the dry fibers. Mechanical stirring was applied for at least 2 h to obtain homogeneous co-dissolved spinning solutions. Before spinning, the solution was stirred until it became clear and was degassed with a SK5200H ultrasonicator (350 W, Shanghai Jinghong Instrument Co., Ltd Shanghai, China) for 15 min.

2.4 Electrospinning

To avoid air bubbles, degassed spinning solutions were carefully loaded into a 5 ml syringe with a stainless steel capillary metal-hub needle with inside diameter at 0.8 mm. Before applying a high voltage power supply (ZGF60 kV/2 mA, Shanghai, China), collector covered with aluminium foil was employed to deposit the electrospun fibers. During the electrospinning, the voltage was kept in 10 kV, and the distance between the needle and collector maintained at 15 cm. The flow rate was controlled at 1.5 ml h^{-1} by means of a single syringe pump (KDS 100, Cole-Parmer, Vernon Hills, IL, USA). After electrospinning, fibers were further dried at 50 °C under vacuum (320 Pa) in a DZF-6050 Electric Vacuum Drying Oven (Shanghai Laboratory Instrument Work Co., Ltd., Shanghai, China) for 24 h to remove residual organic solvents and water.

2.5 Characterization of electrospun nanofibrous membrane

The fiber membranes were cut into 16 cm diameter discs as samples for pharmacotechnical experiments. To ensure a representative count, all the following experiments were carried out in triplicate.

2.5.1 Morphology

The macroscopic morphology and surface texture of electrospun fibers was assessed by Scanning electron microscopy (SEM, JSM-5600LV instrument, JOEL, Tokyo, Japan). Prior to examination, samples were gold sputter-coated under argon to render them electrically conductive. Pictures were then taken at an excitation voltage of 15 kV.

2.5.2 Differential scanning calorimetry analysis

Differential scanning calorimetry (DSC) was measured by means of an MDSC2910 differential scanning calorimeter (TA Instruments Co., New Castle, DE, USA). Sealed samples were heated at 10 K min^{-1} from 50 to 300 °C under nitrogen. The gas flow rate was fixed at 40 ml min^{-1} during the process of analysis.

2.5.3 X-ray diffraction analysis

Wide angle X-ray diffraction (XRD) was obtained by the aid of a D/Max-BR diffractometer (RigaKu, Tokyo, Japan), with Cu Kα radiation in the 2θ range of 5°–60° at 40 mV and 300 mA.

2.5.4 Attenuated total reflectance Fourier transform infrared spectra analysis

Attenuated total reflectance Fourier transform infrared spectra (ATR-FTIR)were obtained on a Nicolet-Nexus 670 FTIR spectrometer (Nicolet Instrument Corporation, Madison, WI, USA) using the KBr disk method (2 mg sample in 200 mg KBr) at the scanning range of 500–4,000 cm^{-1} and a resolution of 2 cm^{-1}.

2.5.5 In vitro dissolution tests

The in vitro dissolution tests were conducted using a ZRS-8G dissolution tester (Tianjin, China) based on the paddle method of Chinese Pharmacopoeia (2005 Edn.). Samples of emodin-loaded nanofibers and pure emodin were immersed in 900 ml normal saline solution (0.9 % NaCl solution) under constant stirring at 37 °C. At certain time intervals, 3 ml solution was taken out of the buffer into test tube with 2 ml NaOH solution (0.025 mol l^{-1}). Then another 3 ml fresh buffer solution was added into the dissolution system. The amount of drug released was determined by a UV spectrophotometer (Unico Instrument, Shanghai, China) at wavelength of 530 nm. The release experiments of each sample were performed in triplicate. Average values of the dissolved drug at specified time periods were plotted as percentage released versus time (min).

2.6 In vivo wound healing test

2.6.1 Animals

All protocols were approved by the Shanghai Jiaotong University Medical Center Institutional Animal Care and Use Committee. 15 male K.M. mice (provided by the Department of Laboratory Animal Science, Shanghai Jiaotong University, Shanghai, China) weighting 24–29 g were used in this study and housed in groups of five animals each, with 12:12 h light–dark cycle and with food and water ad libitum.

2.6.2 Surgical procedure

The previously described protocol to establish mice model of acute full-thickness skin wound was modified in this study. Briefly, mice were anaesthetized with an intraperitoneal injection of ketamine (100 mg kg^{-1}). Their dorsal skins were depilated with 8 % sodium sulfide and swabbed with povidone–iodine followed by 75 % ethanol for three times. On day 0, Two full-thickness round wounds (10 mm of diameter each) were created on the upper back of each mouse. Mice were randomly assigned to three trial groups ($n = 5$ for each group) and were then subjected to different kinds of treatments: (1) receives emodin/PVP blended nanofibrous membrane; (2) receives solo PVP electrospun nanofibrous membrane of the same size; (3) receives no treatment as control group. All wounds were then fixed by sterile Medical Infusion Fixation Paster (RENHE Medical Supplies Company Co., Ltd., Zhejiang, China). Fresh nanofibrous membranes of the same type were reapplied with the change of the Fixation Paster every other day (at even days) in group (1) and (2) while in the control group, only Fixation Paster was changed at same intervals [18–20]. All wounds were photographed from a standard height at odd days.

2.6.3 Wound closure analysis

Three independent, blinded observers evaluated the wound appearances and measured the wound size using planimetric methods (Adobe Photoshop CS5 Software) from the digital photographs taken over a period of 15 days.

The percentage of wound healing is defined as B/A × 100 %, where *A* is the initial wound area and *B* is the wound area after a fixed time interval.

2.6.4 Histological evaluations

On day 15, animals of each group were euthanized. The reconstituted skin was cut to the control depth determined as the layer of panniculus carnosus and harvested including surrounding skin area of 0.5 cm. Samples were fixed with neutral formalin 10 %, embedded in paraffin, and then sectioned with a microtome to obtain 4–5 μm-thick paraffin sections to be stained according to routine Hematoxylin and Eosin (H&E) protocols [21, 22]. Digital images of each H&E stained wound cross sections were prepared. Three independent, blinded observers performed the histological evaluation, parameters such as degree of re-epithelialization, granulation tissue thickness, matrix density, inflammatory cell infiltration, and capillary formation were used to evaluate the degree of wound healing [23, 24].

2.6.5 Statistical analysis

Data were collected from ten samples and were expressed as mean ± standard deviation (SD). Statistical analysis was performed with Student's *t* test and significance was determined at $P < 0.05$.

3 Results and discussion

3.1 Morphology

Surface morphologies of the electrospun PVP nanofiber with or without emodin were shown in Fig. 2. It demonstrated that there were not any visible aggregates separating out from the fiber matrix, suggesting that phase separation had not happened during electrospinning processing. Hence, the system could be termed as nanosolid dispersions. These results validate that our electrospun nanofiber possesses necessary biochemical properties to recruit emodin onto its surface and provides a favorable biophysical environment for the drug to be stably existed [25].

3.2 Differential scanning calorimetry analysis

DSC thermograms are given in Fig. 3. It showed that the pure emodin exhibited a single endothermic response corresponding to the melting of the drug at 257 °C. As an amorphous polymer, PVP K90 did not show any fusion peak or phase transition, apart from a broad endotherm due to dehydration, which lies between 80 and 120 °C. The DSC curve of the medicated nanofiber do not present any melting peak but a broad endotherm ranging from about 70–110 °C, assuming that emodin in the composite fibers has lost its original crystalline state and has been changed into an amorphous state.

3.3 X-ray diffraction analysis

The existence of numerous notable peaks in the XRD spectrum of emodin indicated that raw drug was present in the crystalline form, with the characteristic diffraction peaks appearing at diffraction angles 2θ of 9.76°, 12.92°, 26.08°, and 28.20°. On the contrary, the spectrum of amorphous PVP K90 was characterized by the complete absence of any diffraction peak, suggesting that the molecular orientation and arrangement of the polymer were disordered. Similarly, there are no discrete peaks in the medicated nanofibers, which revealed that drug no longer existed as a crystalline material, and was completely converted into the amorphous state (Fig. 4). All results achieved from the XRD analysis coincided with those from the DSC analysis.

3.4 Attenuated total reflectance Fourier transform infrared spectra analysis

The attenuated total reflectance Fourier transform infrared spectra of PVP, emodin and emodin loaded nanofibers are shown in Fig. 5. As illustrated, the dominant peak of PVP appeared at 1,662 cm^{-1} (C=O stretching), and 2,943 cm^{-1} (C–H stretching). A broad band was also visible at 3,459 and

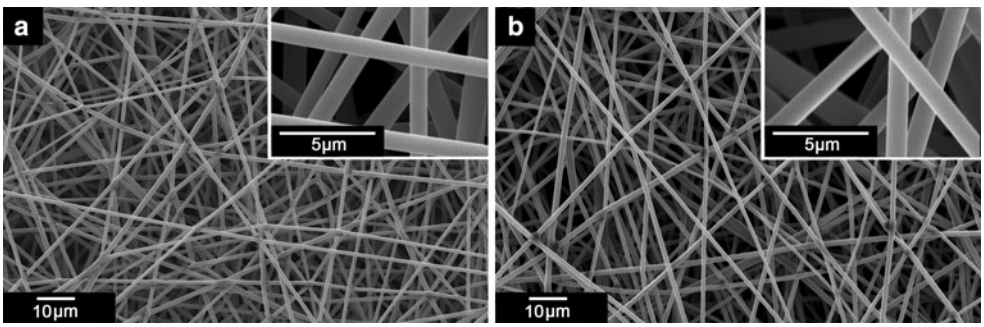

Fig. 2 SEM images: **a** emodin/PVP nanofibers, **b** PVP nanofibers

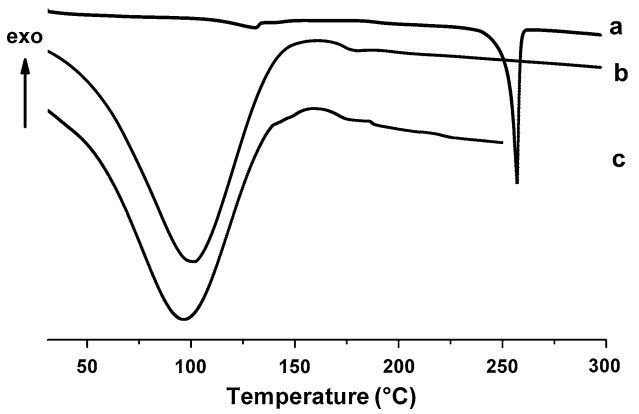

Fig. 3 DSC curves: *a* emodin, *b* emodin/PVP blended nanofiber, *c* PVP nanofiber

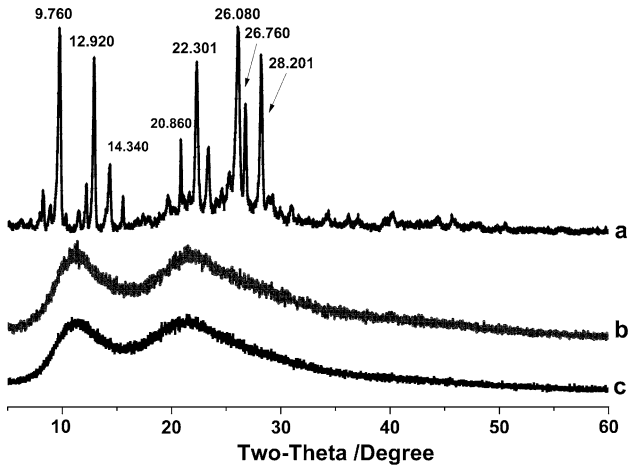

Fig. 4 X-ray diffractograms: *a* emodin, *b* emodin/PVP blended nanofiber, *c* PVP nanofiber

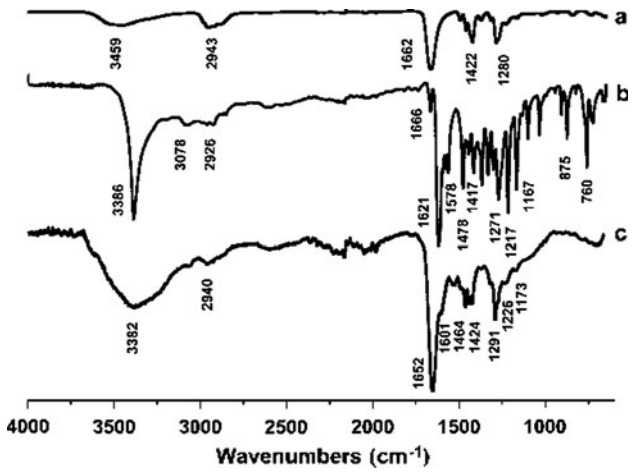

Fig. 5 ATR-FTIR spectra: *a* PVP nanofiber, *b* emodin, *c* emodin/PVP blended nanofiber

3,382 cm^{-1} in PVP and emodin/PVP blended nanofibrous membrane due to the presence of water, causing the broad endotherm detected in the DSC experiments. Two characteristic sharp peaks are visible in the emodin spectrum. One is at 1,621 cm^{-1}, the other at 3,386 cm^{-1}, which is consistent with the standard infrared spectra of this phenolic compound, representing the formation of emodin crystalline. In the spectrum of the medicated fibers, the peak at 1,621 cm^{-1} disappeared, when emodin was incorporated into the electrospun nanofiber. It seems to be the disruption of the interaction between the emodin molecules and the formation of the hydrogen bond between PVP and emodin that made the drug distribute in the polymer composite at a molecular level, not as a dimer crystalline lattice. These interactions also showed the compatibility between drug and polymer composite, and could be favorable to the stability of dispersions of drug in the electrospun matrix.

3.5 In vitro dissolution tests

The release profiles of the pure emodin and emodin from medicated nanofibrous membrane are shown in Fig. 6. It demonstrated a marked improvement of the dissolution rate of emodin in the nanofibrous membranes compared to that of the pure drug. For the membrane, 73.2 % and 96.7 %, respectively, of emodin dissolved in the first 30 and 60 min. After 90 min, nearly all emodin in the membrane was released into the dissolution medium and the exhaustion time for the drug was about 120 min, while at the same time only 4.2 % of the drug was freed from the pure emodin particles. The better dissolution profiles of emodin in the membrane can be partially ascribed to the above-mentioned reasons such as high surface area of the nanofiber material, the

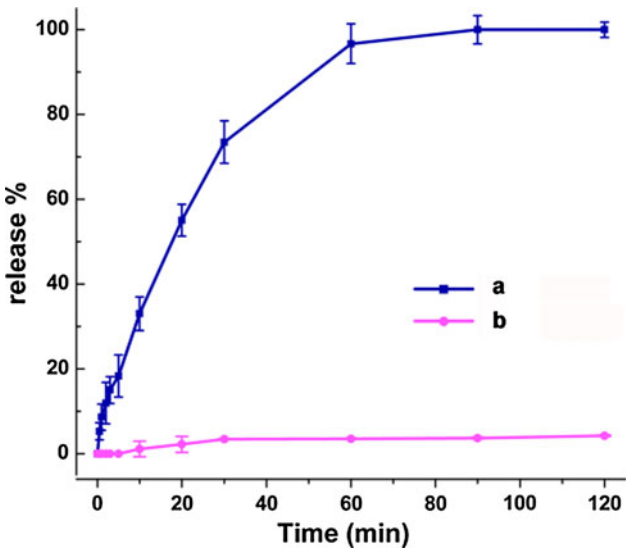

Fig. 6 Dissolution profiles of emodin: *a* emodin/PVP blended nanofiber *b* emodin particles (pure drug)

abundant porosity, and the excellent wettability of PVP, but more importantly, is the enhanced surface area of emodin in the form of nanosolid dispersions and the physical status of the high energy amorphous or molecular form.

3.6 In vivo wound healing test and histological evaluation

Both emodin loaded/non-loaded nanofibrous membranes are quickly attached to the wound surface when applied, and the electrospun nanofiber material has a trend to contract and dissolve under wet conditions. During the experiment, there were no local and systemic adverse reactions such as edema, erythema and skin irritation occurred on the treated mice, indicating that the nanofiber material is highly biocompatible to the wound surface without invoking any cyto-toxic and allergenic effects, and its surface biochemistry is favorable for attachment, which is critical for wound healing. The wound appearance are summarized and shown in Fig. 7a: In the control group, wounds dried faster than those covered by the nanofibrous membranes and newly formed crust were contaminated with dirt and dust which were easily abraded thus creating new wounds. By comparison, wounds treated by emodin loaded nanofibrous membrane showed better fluid retainment, and a continuous re-epithelialization with shrinkage of the wound area was observed. Our findings consist with previous literature that a moist environment helps promote more rapid re-epithelialization [26].

3.6.1 Wound closure analysis

Figure 7b Showed the changes in wound areas at different healing times using emodin/PVP nanofibrous membrane, simple PVP nanofibrous membrane, and none treatment (negative control). All electrospun nanofibrous membranes (with or without emodin) showed a promoted wound healing in 15 days. The wound areas decreased gradually and reached about 5.18 and 9.32 % respectively, on day 15 when electrospun nanofibrous membranes (with or without emodin) were used; whereas in the none treatment group, only 17.28 % of the initial wound area was reached ($P < 0.05$). Therefore, emodin/PVP nanofibrous membrane was found to be better than none treatment ($P < 0.05$) and simple PVP nanofibrous membrane in promoting wound healing (although the difference to the latter was not statistically significant on day 5, 7 and 9). The accelerated wound healing validated our hypothesis that a highly porous structure and a high surface area of nanofiber together with functional pro-healing drug allow the fabricated material to be a vigorous healing accelerator.

3.6.2 Histological evaluations

Accordingly, histological evaluation further confirmed its elevated healing ability 15 days post-wounding. Figure. 8 showed the healing patterns of the treated and untreated samples under histological evaluation. There was a marked infiltration of the inflammatory cells, increased young capillaries and enhanced proliferation of fibroblasts in the emodin/PVP nanofibrous membrane treated group, the wound area was observed to be filled with dense connective tissues (granular layer formation, e). In the control group (a) and the group treated with PVP nanofibrous membrane(c), the inflammatory response and cellular infiltration were observed but less evident, newly formed connective tissues and blood vessels could be found, however, the density of collagen fiber bundles was lower and their distribution was not even (b, d) when compared to that of the medicated fibrous membrane treated group (f) [27]. It is noteworthy that the electrospun nanofibrous

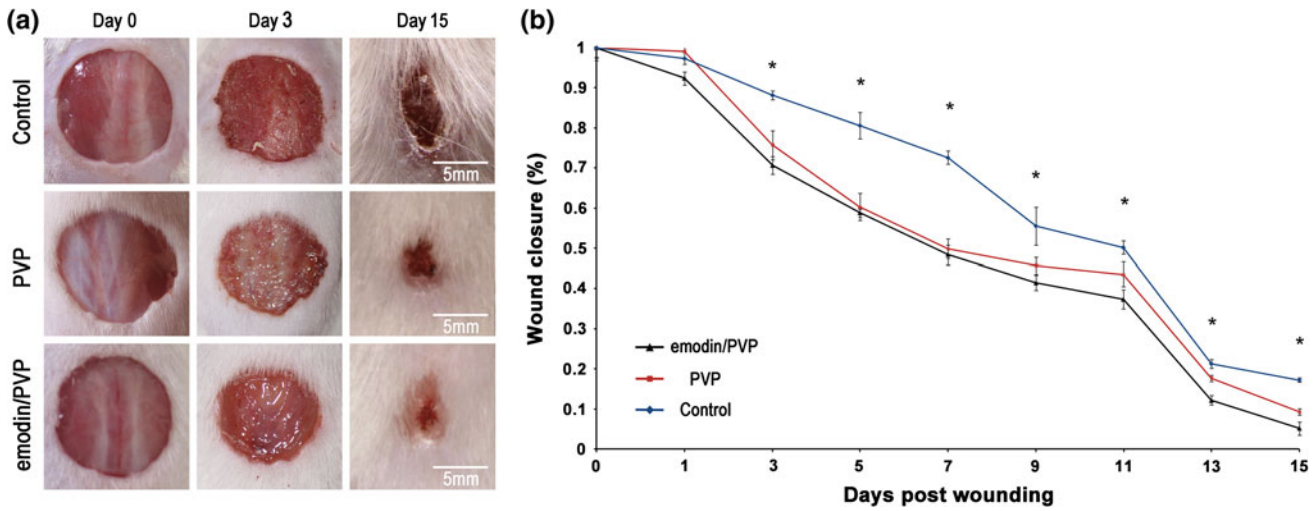

Fig. 7 **a** Wound size and appearances at different time point's **b** wound healing test

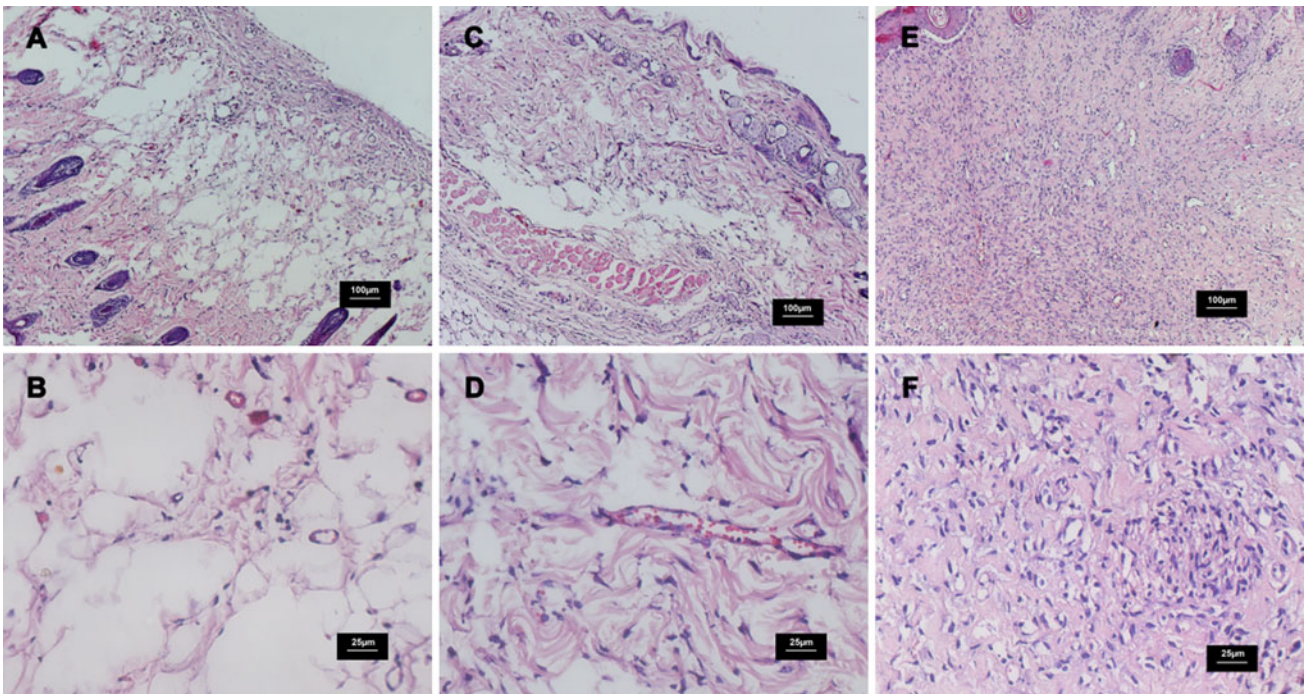

Fig. 8 Histological evaluation with Hematoxylin and Eosin-stain in different groups on day 15. **a**, **b** control; **c**, **d** PVP nanofibrous membrane treated group; **e, f** emodin/PVP nanofibrous membrane treated group. *Scale bars*: (low magnification, 100 μm; high magnification, 25 μm). Collagen fibrils in **e** were spreading into almost all of pores; they were densely-packed and compactly arranged with more fibroblasts cells **f**. However, in **a** and **c**, they were just loosely packed and irregularly arranged with interstices obviously been seen, and wounds were only moderately cellular with fibroblast cells **b, d**. Besides, more capillaries could be found in **e** than that in **a** and **c**

membrane is likely to contract and dissolve in a wet environment, a disadvantage that the membrane has a tendency toward degradation in a short period of time during the in vivo experiment. It might be explained that the ultrafine nanofibrous membrane is insufficient in thickness and do not have support structure to sustain. Although electrospinning of scaffolds thicker than 300 μm is difficult due to current technical limitations, thicker scaffolds, however, could be fabricated by the fine tuning of process parameters [22]. One possible speculation would be that this medicated nanofibrous membrane could be used as a functional constituent to prepare better porous three dimensional dressing material, or even tissue engineered living wound dressing when combined with other selected bioactive scaffold forming materials [28], a simple way to achieve this, presumably, would be the use the of mechanical compression forming technique [29].

4 Conclusion

Emodin could be successfully incorporated into a highly porous nanofibrous membrane. Results from SEM, DSC and XRD adequately demonstrated that emodin was homogenously distributed in the form of amorphous nanosolid dispersions. ATR-FTIR results illustrated that the main interactions between PVP and emodin might be mediated through hydrogen bonding. Drug release test demonstrated its potential as drug delivery systems to largely improve emodin's dissolution profiles. In vivo wound healing test and histological evaluation further showed that the medicated nanofibrous material is nontoxic, nonallergenic and highly biocompatible to the wound surface and its application can accelerate wound healing. Taken together, our study provides evident that the loaded drug retained its biological functionality, suggesting that electrospinning is a good method to incorporate and release drugs in nanofibrous materials, which have the great potential in strategies to develop promising material and drug delivery system for novel therapeutic applications, such as scaffolds for tissue engineering and more specifically, biomedical wound dressings for the acceleration of acute full-thickness skin wounds [8, 30].

References

1. Franz MG, Steed DL, Robson MC. Optimizing healing of the acute wound by minimizing complications. Curr Probl Surg. 2007;44(11):691.
2. Sen CK, Gordillo GM, Roy S, Kirsner R, Lambert L, Hunt TK, et al. Human skin wounds: a major and snowballing threat to public health and the economy. Wound Repair Regen. 2009; 17(6):763–71.

3. Scherer SS, Pietramaggiori G, Matthews J, Perry S, Assmann A, Carothers A, et al. Poly-N-acetyl glucosamine nanofibers: a new bioactive material to enhance diabetic wound healing by cell migration and angiogenesis. Ann Surg. 2009;250(2):322.
4. Katti DS, Robinson KW, Ko FK, Laurencin CT. Bioresorbable nanofiber-based systems for wound healing and drug delivery: optimization of fabrication parameters. J Biomed Mater Res B Appl Biomater. 2004;70B(2):286–96. doi:10.1002/jbm.b.30041.
5. Liu X, Lin T, Fang J, Yao G, Zhao H, Dodson M, et al. In vivo wound healing and antibacterial performances of electrospun nanofiber membranes. J Biomed Mater Res, Part A. 2010;94(2):499–508.
6. Yu DG, Shen XX, Branford-White C, White K, Zhu LM, Annie Bligh S. Oral fast-dissolving drug delivery membranes prepared from electrospun polyvinylpyrrolidone ultrafine fibers. Nanotechnology. 2009;20:055104.
7. Suganya S, Senthil Ram T, Lakshmi BS, Giridev VR. Herbal drug incorporated antibacterial nanofibrous mat fabricated by electrospinning an excellent matrix for wound dressings. J Appl Polym Sci. 2011;121(5):2893–9.
8. Schneider A, Wang XY, Kaplan DL, Garlick JA, Egles C. Biofunctionalized electrospun silk mats as a topical bioactive dressing for accelerated wound heating. Acta Biomater. 2009;5(7):2570–8. doi:10.1016/j.actbio.2008.12.013.
9. Jannesari M, Varshosaz J, Morshed M, Zamani M. Composite poly(vinyl alcohol)/poly (vinyl acetate) electrospun nanofibrous mats as a novel wound dressing matrix for controlled release of drugs. Int J Nanomed. 2011;6:993.
10. Xue L. Progress in the pharmacological study of Chinese herbal drug: polygonum cuspidatum. Zhongguo Zhong yao za zhi=Zhongguo zhongyao zazhi=China. J Chin Mater Med. 2000;25(11):651.
11. Lu HM, Ni WD, Liang YZ, Man RL. Supercritical CO^2 extraction of emodin and physcion from Polygonum cuspidatum and subsequent isolation by semipreparative chromatography. J Sep Sci. 2006;29(14):2136–42.
12. Tang T, Yin LW, Yang J, Shan G. Emodin, an anthraquinone derivative from Rheum officinale Baill, enhances cutaneous wound healing in rats. Eur J Pharmacol. 2007;567(3):177–85. doi:10.1016/j.ejphar.2007.02.033.
13. Bühler V. Polyvinylpyrrolidone excipients for pharmaceuticals: povidone, crospovidone, and copovidone. Heidelberg, Germany: Springer; 2005.
14. Fischer F, Bauer S. Polyvinylpyrrolidon. Ein Tausendsassa in der Chemie. Chem unserer Zeit. 2009;43(6):376–83.
15. Yu D, Shen X, Zhang X, Branford-White C, Zhu L. Preparation and characterization of fast-dissolving electrospun drug-loaded nanofiber membrane. Acta Polymerica Sinica. 2009;11:88–92.
16. Nie W, Yu DG, Branford-White C. Electrospun zein–PVP fibre composite and its potential medical application. Mater Res Innovations. 2011;16(1):14–8.
17. Wang H, Dong Y, Xiu ZL. Microwave-assisted aqueous two-phase extraction of piceid, resveratrol and emodin from Polygonum cuspidatum by ethanol/ammonium sulphate systems. Biotechnol Lett. 2008;30(12):2079–84.
18. Rho KS, Jeong L, Lee G, Seo BM, Park YJ, Hong SD, et al. Electrospinning of collagen nanofibers: effects on the behavior of normal human keratinocytes and early-stage wound healing. Biomaterials. 2006;27(8):1452–61.
19. Chen JP, Chang GY, Chen JK. Electrospun collagen/chitosan nanofibrous membrane as wound dressing. Colloids Surf A. 2008;313:183–8. doi:10.1016/j.colsurfa.2007.04.129.
20. Ma K, Liao S, He L, Lu J, Ramakrishna S, Chan CK. Effects of nanofiber/stem cell composite on wound healing in acute full-thickness skin wounds. Tissue Eng Part A. 2011;17(9–10):1413–24. doi:10.1089/ten.TEA.2010.0373.
21. Slaoui M, Fiette L. Histopathology procedures: from tissue sampling to histopathological evaluation. Methods Mol Biol (Clifton, N.J.). 2011;691:69.
22. Babaeijandaghi F, Shabani I, Seyedjafari E, Naraghi ZS, Vasei M, Haddadi-Asl V, et al. Accelerated epidermal regeneration and improved dermal reconstruction achieved by polyethersulfone nanofibers. Tissue Eng Part A. 2010;16(11):3527–36. doi:10.1089/ten.TEA.2009.0829.
23. Erba P, Adini A, Demcheva M, Valeri CR, Orgill DP. Poly-N-acetyl glucosamine fibers are synergistic with vacuum-assisted closure in augmenting the healing response of diabetic mice.J Trauma. 2011;71(2):S187.
24. Tsuboi R, Rifkin DB. Recombinant basic fibroblast growth factor stimulates wound healing in healing-impaired db/db mice. J Exp Med. 1990;172(1):245–51.
25. Zhang X, Thomas V, Xu Y, Bellis SL, Vohra YK. An in vitro regenerated functional human endothelium on a nanofibrous electrospun scaffold. Biomaterials. 2010;31(15):4376–81. doi:10.1016/j.biomaterials.2010.02.017.
26. Janis JE, Kwon RK, Lalonde DH. A practical guide to wound healing. Plast Reconstr Surg. 2010;125(6):230e.
27. Kang YO, Yoon IS, Lee SY, Kim DD, Lee SJ, Park WH, et al. Chitosan-coated poly(vinyl alcohol) nanofibers for wound dressings. J Biomed Mater Res B Appl Biomater. 2010;92(2):568–76.
28. Franco RA, Nguyen TH, Lee BT. Preparation and characterization of electrospun PCL/PLGA membranes and chitosan/gelatin hydrogels for skin bioengineering applications. J Mater Sci Mater Med. 2011;22(10):1–12.
29. Ananta M, Mudera V, Brown RA. A rapid fabricated living dermal equivalent for skin tissue engineering: an in vivo evaluation in an acute wound model. Tissue Eng. 2011;18(3–4):353–61.
30. Zhong S, Zhang Y, Lim C. Tissue scaffolds for skin wound healing and dermal reconstruction. Interdiscip Rev Nanomed Nanobiotechnol. 2010;2(5):510–25.